International Journal of Thermophysics, Vol. 16, No. 1, 1995

Hyperbaric Reservoir Fluids: High-Pressure Phase Behavior of Asymmetric Methane + *n*-Alkane Systems[1]

E. Flöter,[2] Th. W. de Loos,[2,3] and J. de Swaan Arons[2]

In this paper, experimental three-phase equilibrium (solid *n*-alkane + liquid + vapor) data for binary methane + *n*-alkane systems are presented. For the binary system methane + tetracosane, the three-phase curve was determined based on two phase equilibrium measurements in a composition range from $x_{C24} = 0.0027$ to $x_{C24} = 1.0$. The second critical endpoint of this system was found at $p = (104.7 \pm 0.5)$ MPa, $T = (322.6 \pm 0.25)$ K, and a mole fraction of tetracosane in the critical fluid phase of $x_{C24} = 0.0415 \pm 0.0015$. The second critical endpoint occurs where solid tetracosane is in equilibrium with a critical fluid phase ($S_{C24} + L = V$). For the binary systems of methane with the *n*-alkanes tetradecane, triacontane, tetracontane, and pentacontane, only the coordinates of the second critical endpoints were measured. The second critical endpoint temperature is found close to the atmospheric melting point temperature of the *n*-alkane. The pressures at the second critical endpoints do not exceed 200 MPa. Based on these experimental data and data from the literature, correlations for the pressure, temperature, and fluid phase composition at the second critical endpoint of binary methane + *n*-alkane systems with *n*-alkanes between octane and pentacontane were developed.

KEY WORDS: correlation; methane + *n*-alkane; second critical endpoint; three-phase curve.

1. INTRODUCTION

The phase behavior of binary systems containing methane and a higher *n*-alkane is of particular interest for the production and processing of oil

[1] Paper presented at the Twelfth Symposium on Thermophysical Properties, June 19–24, 1994, Boulder, Colorado, U.S.A.

[2] Laboratory of Applied Thermodynamics and Phase Equilibria, Faculty of Chemical Engineering and Materials Science, Delft University of Technology, Julianalaan 136, 2628 BL Delft, The Netherlands.

[3] To whom correspondence should be addressed.

0195-928X/95/0100-0185$07.50/0

and natural gas. These mixtures are also of special interest because of their rather large deviations from ideal behavior at elevated pressures. These nonidealities are caused mainly by the size differences of the components.

The type of phase behavior of methane + n-alkane systems changes systematically with increasing chain length of the n-alkane [1–3]. Systems of methane and octane or higher n-alkanes only show three-phase curves involving a solid heavy n-alkane (S_{CN}), a liquid, and a vapor phase ($S_{CN}LV$). In all these systems, first and second critical endpoints ($S_{CN} + L = V$) occur. A critical fluid phase is in equilibrium with the solid heavy n-alkane at these critical endpoints. As shown in Fig. 1, the high-temperature branch of the three-phase curve ($S_{C24}LV$), for the methane + tetracosane system, starts at the triple point of the n-alkane. Its pressure

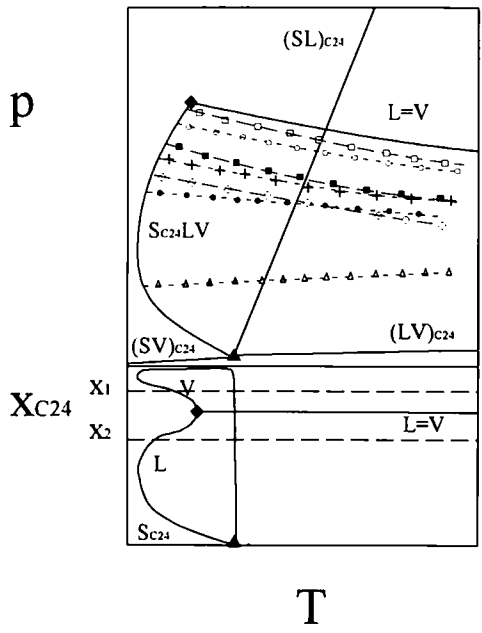

Fig. 1. Schematic depiction of the high-temperature branch of the three-phase curve ($S_{C24}LV$) in a p–T and a corresponding x_{C24}–T projection. (▲) Triple-point tetracosane; (◆) second critical endpoint. Schematic bubble points for fixed compositions: (○) x_1, (+) x_2, (●) x_3, and (△) x_4, with $x_1 < x_2 < x_3 < x_4$. Schematic dew points for fixed compositions: (□) y_1, (■) y_2, and (▽) y_3, with $y_1 > y_2 > y_3$.

maximum is reached at the second critical endpoint, where the three-phase curve ($S_{C24}LV$) is intercepted by the vapor–liquid critical curve. The vapor–liquid critical curve ends in the critical point of the pure heavy *n*-alkane. This kind of phase behavior is, for example, found for the systems methane + hexadecane [4] and methane + eicosane [5].

Knowledge of the coordinates of the second critical endpoint allows estimates of the extension of the vapor–liquid two-phase region of systems of methane and *n*-alkanes with a carbon number higher than seven. In this paper, experimental data for the $S_{C24}LV$ curve in the system methane + tetracosane are presented. These results are compared with literature data for the system methane + hexadecane [4] and methane + eicosane [5].

Furthermore, the coordinates of the second critical endpoint for the binary systems methane + tetradecane, + triacontane, + tetracontane, and + pentacontane are determined experimentally. Also, a correlation for the coordinates of the second critical endpoint for different methane + *n*-alkane systems is presented.

2. EXPERIMENTS

The methane used in this work was of a stated purity of 99.995% (w/w) and was supplied by Air Products. The *n*-alkanes were tetracosane of a purity >99% (w/w) supplied by Janssen and tetracontane (purity, >98%, w/w), triacontane, pentacontane, and tetradecane (all of a purity >99%, w/w) supplied by Fluka. All chemicals were used without further purification.

The experimental procedure is the synthetic method and involves the visual determination of phase boundaries for mixtures of constant and known composition. Different autoclaves were used to perform the measurements. A detailed description of the equipment and the experimental procedure can be found elsewhere [5–7].

Points of the three-phase curve ($S_{CN}LV$) are determined mainly indirectly by the intersection of a vapor–liquid boundary curve with the solid–liquid or solid–vapor boundary curve of the same composition. The solid + fluid/fluid boundary curve and the vapor + liquid/liquid boundary curve are, in a p–T section, almost perpendicular to each other. This yields uncertainties of better than ±0.4 MPa in pressure and ±0.3 K in temperature and ±0.005 in composition. The uncertainty in composition tends to decrease with decreasing mole fraction of the heavy *n*-alkane x_{CN}.

The coordinates of the second critical endpoint ($S_{CN} + L = V$) for the methane + *n*-alkane systems are also evaluated indirectly. The composition of the critical fluid phase present at the second critical endpoint is located

between two different compositions. One composition shows bubble-point behavior and the second one shows dew-point behavior. If these two samples do not differ much in compositions, their coordinates at the three-phase points ($S_{CN}LV$) should have no significant differences. The second critical endpoint is equivalent to the relatively flat local maximum which the three-phase curve ($S_{CN}LV$) has in its p–x and T–x projections. This means that these coordinates are nearly equal to the coordinates of the second critical endpoint ($S_{CN} + L = V$). The resulting uncertainties of the coordinates of the second critical endpoints do not exceed ± 0.75 MPa, ± 0.4 K, and in the mole fraction of the critical fluid phase ± 0.004.

3. RESULTS

The coordinates of the three-phase points found in the system methane + tetracosane are listed in Table I and shown in Fig. 2. For comparison, the three-phase curves of the systems methane + hexadecane [4] and methane + eicosane [5] are also included. All three curves reveal a clear temperature minimum. In all three systems, this temperature minimum occurs at a pressure of about 30 MPa. Because of the shape of the three-phase curve the fluid region of the systems is extended to temperatures clearly below the triple-point temperature of the pure heavy component. This extension is the largest for the methane + hexadecane system. The shape of the three-phase curves can be understood by considering the competing phenomena of freezing-point depression and the increase in the melting-point temperature of the pure n-alkanes with increasing pressure. The different slopes of the three-phase curves in their upper part can be

Table I. Coordinates of Three-Phase Points ($S_{C24}LV$) of the System Methane + Tetracosane

T (K)	p (MPa)	$10^2 x_{C24}$	T (K)	p (MPa)	$10^2 x_{C24}$
319.95[a]	67.00	0.270	318.93	45.89	25.55
321.70[a]	92.50	0.977	318.50	36.72	30.21
322.39[a]	102.01	0.194	318.30	28.55	35.85
322.50[a]	104.06	3.220	318.60	19.02	45.07
322.62	104.33	4.31	319.37	12.15	55.49
322.50	104.06	5.20	319.92	8.10	65.13
322.48	102.50	6.79	321.01	5.05	75.18
321.70	92.80	10.35	322.62	1.93	90.02
320.33	71.73	16.40	323.45	~0	100

[a] Indicates points based on dew-point measurements.

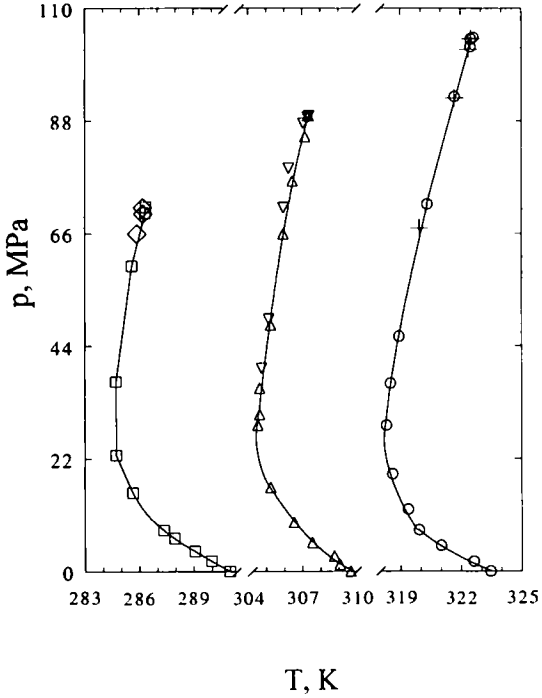

Fig. 2. p T projection of three-phase points ($S_{CN}LV$) of methane + n-alkane systems. Based on bubble points: (□) C_{16}; (△) C_{20}; ( ) C_{24}. Based on dew points: (·) C_{16}; (△) C_{20}; (+) C_{24}. Lines drawn to match the points.

related to the slopes of the respective pure n-alkane melting curves. With the increasing asymmetric nature of the system, the maximum pressure of the three-phase curve is increasing.

Figure 3 shows a reduced pressure (p_r) versus volume fraction of the n-alkane (ϕ^*_{CN}) projection of three-phase curves of different methane + n-alkane systems. The pressures are reduced by the second critical endpoint pressure of the system under consideration. The volume fraction can be evaluated based on van der Waals volumes according to Bondi [8].

As Fig. 3 reveals, the reduced projections of the three-phase curves of the binary systems methane + hexadecane, + eicosane, and + tetracosane almost coincide. It must be noted that as a consequence of the conversion from mole fraction x_{CN} to volume fraction ϕ^*_{CN}, the relative uncertainties change. Especially for low mole fractions of high n-alkanes, the uncertainty of the mole fraction results in a dramatically higher uncertainty of the

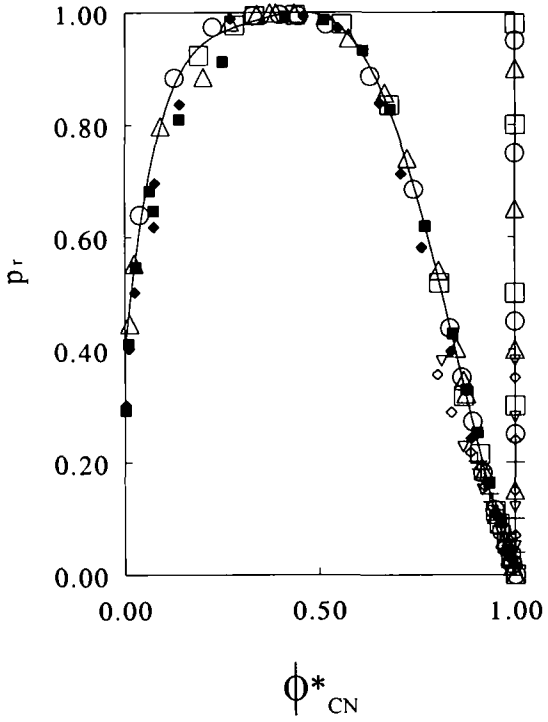

Fig. 3. p_r–ϕ^*_{CN} projection of three-phase curves ($S_{CN}LV$) of methane + *n*-alkane systems. (○) C_{24}; (△) C_{20}; (□) C_{16}; (+) C_{10}; (▽) C_9; (◇) C_8; (■) VLE methane + decane at 263.15 K; (◆) VLE methane + docosane at 263.15 K. Line drawn to match the systems of C_{24}, C_{20}, and C_{16}.

volume fraction. For the systems of methane with octane [9, 10], nonane [11], and decane [12–16], only parts of the three-phase curves were measured. The pressures of these incomplete data sets were reduced with second critical endpoint pressures of the systems of interest, which were relatively uncertain. Considering this, Fig. 3 shows that the data points for these three systems fall on the same master curve.

Complete data sets of three-phase curves of the methane + *n*-alkane systems are scarce. However, for the asymmetric systems investigated isothermal vapor–liquid envelopes, at temperatures close to the pure heavy component triple-point temperature, do not differ too much from p–x projections of the three-phase curves. This allows us to approximate the reduced pressure–volume fraction projections of the three-phase curve ($S_{CN}LV$) of a system by a similar representation of a vapor–liquid envelope. The reduced isothermal ($T = 263.15$ K) vapor–liquid envelopes of

the systems methane + decane [16] and methane + dodecane [17] are, as an approximation of the three-phase curves of these systems, included in Fig. 3. The pressures of the vapor–liquid boundary curves were reduced with the vapor–liquid critical pressure at this temperature. Also, these curves fall on the same master curve.

The coordinates of the second critical endpoint of different methane + *n*-alkane systems determined in this work are listed in Table II. Also, the coordinates of the second critical endpoint of methane + *n*-alkane systems derived from or given in the literature [4, 5, 9–17] are included. With increasing carbon number of the *n*-alkane, the pressure of the second critical endpoint ($S_{CN} + L = V$) increases, while the mole fraction of the *n*-alkane x_{CN} in the critical fluid phase decreases. The temperature coordinate of the second critical endpoint has to be considered in relation to the atmospheric melting point or the triple-point temperature of the pure *n*-alkane. Relative to the pure *n*-alkane atmospheric melting point, the temperature of the second critical endpoint increases with increasing chain length. For carbon numbers of 30 and higher, the second critical endpoint temperature is even higher than the normal melting-point temperature of the pure *n*-alkane.

Table II. Coordinates of the Second Critical Endpoint of Different Methane + *n*-Alkane Systems[a]

n[b]	$10^2 x_{CN}$	$10^2 \delta x_{CN}$	$T_{2nd\ CEP}$ (K)	ΔT (K)	δT (K)	$p_{2nd\ CEP}$ (MPa)	δp (MPa)
8[A*]	10	−1.03	201	−15.39	−0.57	20.3	−0.22
9[B*]	9.5	−0.69	206.2	−13.46	−0.19	26.7	−1.76
10[C*]	9.2	−0.37	232	−11.45	0.47	37	1.23
12[D*]	8.5	0.01	254	−9.56	−0.14	50.6	1.73
14	7.35 ± 0.40	0.02	272.2 ± 0.40	−6.81	0.49	59.75 ± 0.75	−0.68
16[E]	6.6	0.09	286.4	−4.92	0.55	71.5	0.70
20[F]	4.90 ± 0.12	−0.06	307.37 ± 0.15	−2.22	0.27	89.0 ± 0.25	−0.07
24	4.15 ± 0.15	0.02	322.6 ± 0.25	−0.85	−0.70	104.7 ± 0.50	0.18
30	3.05 ± 0.20	−0.05	340.6 ± 0.40	1.95	−0.59	124.2 ± 0.50	−0.32
40	2.05 ± 0.20	−0.07	359.5 ± 0.40	6.35	0.62	152.5 ± 0.50	0.35
50	1.70 ± 0.15	0.04	373.4 ± 0.40	7.75	−0.20	174.7 ± 0.50	−0.25

[a] (n) carbon number; (x_{CN}) mole fraction of the heavy *n*-alkane in the critical fluid phase at the second critical endpoint; (δx_{CN}) its deviation from Eq. (3) based on volume fractions ϕ^*_{CN}; ($T_{2nd\ CEP}$) second critical endpoint temperature; (ΔT) its difference from T_{NMP} of the pure *n*-alkane; (δT) deviation of ΔT from Eq. (2); ($p_{2nd\ CEP}$) second critical endpoint pressure and its deviation (δp) from Eq. (1).

[b] Superscripts indicate references as follows: [A] [9, 10]; [B] [11]; [C] [12–16]; [D] [17]; [E] [14]; [F] [5]; * points based on wide extrapolations.

4. DISCUSSION

The type of phase behavior found for the system methane + tetracosane follows the systematic pattern found for the methane + *n*-alkane family. It was found that the three-phase curve reveals a temperature minimum at $T = (318.3 \pm 0.15)$ K at a pressure of $p = (29 \pm 4)$ MPa. The composition at this temperature minimum is $x_{C24} = 0.358 \pm 0.035$ in the liquid phase and less than $x_{C24} = 0.002$ in the vapor phase. The second critical endpoint ($S_{C24} + L = V$) was found at $x_{C24} = 0.0415 \pm 0.0015$, $T = (322.6 \pm 0.25)$ K, and $p = (104.7 \pm 0.5)$ MPa.

As expected the effects of the asymmetric nature of the methane + *n*-alkane systems are more pronounced for a higher carbon number of the *n*-alkanes. With increasing size of the *n*-alkane, the second critical endpoint pressure increases and the mole fraction of the *n*-alkane in the critical fluid phase at the second critical endpoint decreases. For the three coordinates of the second critical endpoint ($S_{CN} + L = V$) of the different methane + *n*-alkane systems, correlations incorporating only pure-component properties of the *n*-alkane were developed. It is found that the pressure at the second critical endpoint $p_{2nd\ CEP}$ is linearly dependent on the carbon number n of the *n*-alkane to the power 0.25; see Eq. (1).

$$p_{2nd\ CEP} = -245.2 + 158n^{0.25} \tag{1}$$

The deviations between the experimental points and the values given by the correlation are listed in Table II in column δp.

The difference ΔT between the temperature of the second critical endpoint and the atmospheric melting point of the pure *n*-alkane $T_{NMP,CN}$ can be correlated with the logarithm of the critical pressure of the pure *n*-alkane $p_{C,CN}$ (in MPa); see Eq. (2).

$$\Delta T = T_{2nd\ CEP} - T_{NMP,CN} = 0.11 - 16.2 \ln(p_{C,CN}) \tag{2}$$

In Table II the temperature difference ΔT and its deviation δT from the linear correlation Eq. (2) are listed. The relatively large deviations can be explained partly by the uncertainties of the pure-component atmospheric melting temperatures of the heavy *n*-alkanes. The critical pressures used were obtained from the correlations given by Tsonopolous and Tan [18].

It might be seen as a contradiction to the congruence found for the $p_r - \phi^*_{CN}$ projections of the three-phase curves that the volume fraction ϕ^*_{CN} at the second critical endpoint decreases slightly with carbon number. Between the systems methane + tetradecane and methane + pentacontane, it changes from $\phi^*(C_{14}) = 0.41 \pm 0.02$ to $\phi^*(C_{50}) = 0.34 \pm 0.02$. A linear relation between the composition of the critical fluid phase at the second

critical endpoint in terms of the volume fraction $\phi^*_{2\text{nd CEP,CN}}$ of the *n*-alkane and the carbon number n is found; see Eq. (3).

$$\phi^*_{2\text{nd CEP,CN}} = 0.438 - 0.0021n \tag{3}$$

This correlation [Eq. (3)] is developed based only on data of the systems incorporating a heavy *n*-alkane equal or higher than dodecane. In Table II the deviations δx_{CN} in mole fraction between the experimental values and the correlation results are listed. The given mole fractions of the fluid phase at the second critical endpoint for the systems of methane with octane and with nonane are highly uncertain because they are based on rather wide extrapolations.

It can be concluded that the linear correlations developed for the coordinates of the second critical endpoint of methane + *n*-alkane systems are in good agreement with the experimental results reported in this paper and the ones found in the literature. For different methane + *n*-alkane systems, with *n*-alkanes between octane and pentacontane, the correlations reproduce and predict the coordinates of the second critical endpoint within the experimental uncertainties.

The coordinates of the second critical endpoint of methane + *n*-alkane systems contain valuable information. First, the pressure coordinate of the second critical endpoint, for systems with $n \geqslant 12$ [17], is the absolute pressure maximum of the vapor–liquid two-phase region of this system. This is so because the vapor–liquid critical curve has a negative slope $(\partial p/\partial T)_{L=V}$. The composition of the critical fluid phase along the vapor–liquid critical curve changes less with temperature for more asymmetric methane + *n*-alkane systems. This means that $(\partial x/\partial T)_{L=V}$ becomes smaller with increasing chain length of the *n*-alkane. For example, in the system composed of methane + tetracosane, the difference between the vapor–liquid critical composition, at temperatures up to 150 K higher than the second critical endpoint temperature, and the composition of the critical fluid phase at the second critical endpoint is less than 0.0025. So we can conclude that knowledge of the composition of the critical fluid phase in the second critical endpoint allows us to estimate whether a mixture of a given composition will reveal dew points or bubble points. For a mixture mole fraction of the heavy *n*-alkane smaller than at the second critical endpoint, as indicated by x_1 in Fig. 1, the mixture is a homogeneous vapor phase for pressures higher than the vapor–liquid envelope pressures. For the composition x_2 in Fig. 1, indicating a mixture mole fraction of the heavy *n*-alkane larger than at the second critical endpoint, the homogeneous phase at pressures higher than the vapor–liquid envelope pressures is a liquid.

REFERENCES

1. J. S. Rowlinson and F. L. Swinton, *Liquids and Liquid Mixtures*, 3rd ed. (Butterworth, London, 1982).
2. A. J. Davenport and J. S. Rowlinson, *Trans. Faraday Soc.* **59**:78 (1963).
3. J. P. Kohn, *AIChE J.* **7**:514 (1961).
4. M. Glaser, C. J. Peters, H. J. van der Kooi, and R. N. Lichtentaler, *J. Chem. Thermodyn.* **17**, 803 (1985).
5. H. J. van der Kooi, E. Flöter, and Th. W. de Loos, submitted for publication.
6. Th. W. de Loos, H. J. van der Kooi, and P. L. Ott, *J. Chem. Eng. Data* **31**:166 (1986).
7. Th. W. de Loos, A. J. M. Wijen, and G. A. M. Diepen, *J. Chem. Thermodyn.* **12**:193 (1980).
8. A. Bondi, *Physical Properties of Molecular Crystals, Liquids and Glasses* (Wiley, New York, 1968), pp. 450–453.
9. J. P. Kohn and W. F. Bradish, *J. Chem. Eng. Data* **9**:5 (1964).
10. J. P. Kohn, K. D. Luks, P. H. Liu, and D. L. Tiffin, *J. Chem. Eng. Data* **22**:419 (1977).
11. L. M. Shipman and J. P. Kohn, *J. Chem. Eng. Data* **11**:176 (1966).
12. J. M. Beaudoin and J. P. Kohn, *J. Chem. Eng. Data* **12**:189 (1967).
13. H. H. Reamer, R. H. Olds, B. H. Sage, and W. N. Lacey, *Ind. Eng. Chem.* **34**:1526 (1942).
14. H. C. Wiese, H. H. Reamer, and B. H. Sage, *J. Chem. Eng. Data* **15**:75 (1970).
15. F. I. Stalkup and R. Kobayashi, *AIChE J.* **9**:121 (1963).
16. M. P. W. M. Rijkers, M. Malais, C. J. Peters, and J. de Swaan Arons, *Fluid Phase Equil.* **71**:143 (1992).
17. M. P. W. M. Rijkers, V. B. Maduro, C. J. Peters, and J. de Swaan Arons, *Fluid Phase Equil.* **72**:309 (1992).
18. C. Tsonopoulos and Z. Tan, *Fluid Phase Equil.* **83**:127 (1993).